THE INFLUENCE OF ANNEALING ON SELECTED MECHANICAL PROPERTIES OF PETG PRINTS PRODUCED BY FDM

MARCIN MACINIAK[1], JACEK OCHOROK[1]

[1]The Faculty of Mechanics and Technology in Stalowa Wola, Rzeszów University of Technology,

Kwiatkowskiego 4, 37-450 Stalowa Wola, Poland

DOI: 10.17973/MMSJ.2026_11_2026096

e-mail m.marciniak@prz.edu.pl

This study examines the effect of annealing on the mechanical properties, deformation behaviour, and fracture mechanisms of PETG specimens fabricated using Fused Deposition Modelling (FDM). Samples with infill densities of 25%, 50%, 75%, and 100% were subjected to thermal treatment at 90°C, 100°C, and 110°C, followed by controlled cooling conditions.

Mechanical performance was evaluated using tensile testing, while deformation processes were analysed via infrared thermography. The results demonstrate that annealing significantly influences strength, structural integrity, and failure behavior, with optimal performance observed near the glass transition temperature. The findings highlight the critical role of thermal post-processing in enhancing the performance of additively manufactured polymer components

KEYWORDS

Additive manufacturing, FDM, PETG, annealing, tensile properties, infill density,

1 INTRODUCTION

One of the widely used materials in FDM/FFF additive manufacturing technology is PETG (polyethylene terephthalate glycol-modified). This material is an evolution of the classic PET, known from the packaging industry, among others; however, the application of glycol modification leads to a reduction in material crystallization, thereby improving its processability in the 3D printing process [Wohlers 2022, Styp 2020].

PETG is classified as an amorphous thermoplastic, which results in low processing shrinkage and good dimensional stability of finished components [Adamczyk 2020]. Compared to the popular PLA, this material is characterized by significantly higher impact resistance and lower brittleness, which ensures that manufactured parts exhibit greater operational durability [Duda 2016]. At the same time, PETG maintains a relatively simple printing process that does not require a closed build chamber, making it attractive for both prototyping and utility applications.

In terms of thermal properties, PETG exhibits higher resistance to elevated temperatures than PLA, reaching a heat deflection temperature of approximately 70–80°C [Przybylski 2020, PETG 2026]]. Although this value is lower than that of ABS or polyamides, it proves sufficient for many structural and functional components [Ngo 2018]. An additional advantage of the material is its good chemical resistance, covering contact with water, oils, alcohols, and selected chemical substances, which enables the use of prints in environments with high humidity.

The PETG printing process is typically carried out within a nozzle temperature range of 220 to 250°C and a heated bed temperature of 70 to 90°C [[ASTM 2009], [Mikos 2021]]. This material features very good interlayer adhesion, which positively influences the mechanical strength of elements in the Z-axis [Ngo 2018]. At the same time, excessive cooling can lead to a deterioration in the quality of layer bonding; therefore, the use of moderate cooling fan speed is recommended [Gibson 2021]. Characteristic technological challenges of PETG include a tendency for "stringing" and increased melt viscosity, which require proper calibration of retraction parameters [PETG 2026].

Due to its properties, PETG is widely used in the manufacturing of housings, brackets, structural elements, and parts used in outdoor conditions [Ngo 2018, Duda 2016]. The availability of transparent variants further expands its range of applications in aesthetic and functional components where partial light transmission is important [Przybylski 2020]. In literature, PETG is indicated as a compromise material, combining ease of processing with favorable mechanical and chemical properties [Gibson 2021].

Strength testing of components manufactured using the Fused Deposition Modelling (FDM) method plays a key role in analysing the influence of the structure of additively manufactured material on its mechanical properties [AutomatykaOnline 2021]. A particularly important issue is the way forces propagate in samples printed from PETG, a thermoplastic material with high chemical resistance and good thermal-mechanical stability [Gorczynska 2018].

A static tensile test, performed in accordance with the principles accepted in classical mechanics of materials and AM normative terminology [ASTM 2009], [ASTM/ISO 2021], enables the observation of processes responsible for the deformation and failure of layer-printed material. In the case of FDM samples, their anisotropic, layered structure—resulting from the direction of the toolpaths and the quality of interlayer adhesion—plays a crucial role [Szykiedans 2016].

In the initial phase of loading, forces are primarily transferred by continuous infill paths oriented along the direction of the applied load. However, due to the microstructure of the material—the presence of pores, geometric discontinuities, and variable effective thickness of the paths—the stress distribution is not homogeneous from the very beginning [Ngo 2018], [Gorczynska 2018, Szykiedans 2016]. This phenomenon is typical for FDM technology, where mechanical properties in the XY-axis differ significantly from those in the Z-axis [Szymczyk 2017].

Thermographic imaging serves as an excellent tool to support the analysis of these processes. Thermal images recorded during a tensile test allow for the observation of local temperature changes resulting from intense deformation work, internal friction, and micro-cracking of the material [Ngo 2018], [Gorczynska 2018]. Bright areas indicate energy concentration—both mechanical and thermal—which correlates with the locations of the highest stress increase. The zones of highest temperature visible on the thermogram coincide with the dominant direction of the infill paths, which clearly confirms the anisotropic nature of load propagation [Szykiedans 2016, Szymczyk 2017].

Annealing (heat treatment) is one of the most important post-processing methods used after manufacturing components with FDM technology. The goal of this process is to improve the quality and durability of prints through controlled thermal exposure, which allows for the reduction of imperfections resulting from the nature of layered printing. During printing, successive layers of material are locally heated and then rapidly cooled, which leads to the formation of residual stresses,

incomplete interlayer bonding, and local structural inhomogeneities [Adamczyk 2020, Ngo 2018]]. Annealing allows these phenomena to be mitigated.

The main objective of annealing is to reduce internal stresses that arise due to uneven temperature gradients during the deposition of subsequent material layers. These stresses can cause cracks, deformations, or reduced resistance to operational loads. Under the influence of a properly selected temperature, the material gains greater mobility of its polymer chain segments, allowing stresses to relax and the structure to stabilize [Przybylski 2020, Gorczynska 2018].

The second significant goal is to improve interlayer adhesion, i.e., strengthening the connections between successive material paths. Under elevated temperature conditions, partial diffusion of polymer chains occurs between adjacent layers (Fig. 1), which increases the degree of their coalescence and, consequently, improves the mechanical strength of the model, especially in the direction perpendicular to the layers [Ngo 2018].

Polyethylene terephthalate (PET) can exhibit either an amorphous or a semi-crystalline structure, depending on its composition and processing conditions. PETG, a glycol-modified variant of PET, is predominantly amorphous due to the disruption of regular chain packing caused by the glycol modification. Consequently, changes in the mechanical properties of PETG during annealing should not automatically be attributed to an increase in crystallinity; structural relaxation and the release of residual stresses may also contribute to the observed changes [Sikora 2006, Wrobel 2019].

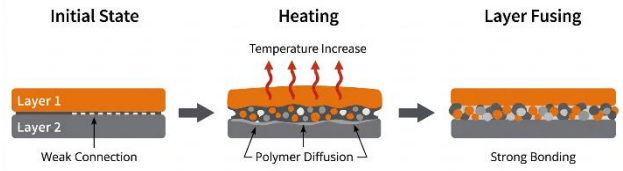


Figure 1. Simplified diagram of the interlayer bonding process [own study]

The mechanism of annealing therefore involves several interdependent phenomena: Relaxation of internal stresses, Diffusion and welding of layers at the molecular level, Reconstruction of the crystalline structure for certain polymers.

The combination of these effects ensures that components subjected to annealing are characterized by greater stability, homogeneity, and mechanical strength. However, the final effectiveness of the process depends on the correct selection of parameters, such as temperature, time, and cooling method, which must be appropriately adapted to the properties of the specific material [Przybylski 2020, Gorczynska 2018].

Annealing is a process that significantly affects the mechanical properties of components manufactured using the FDM method. These changes result primarily from the influence of temperature on the polymer structure, as well as from the mitigation of imperfections characteristic of the layer-based printing process. Literature emphasizes that a properly selected annealing process can significantly improve the performance of prints under operational loads [Szymczyk 2017].

One of the most important effects of annealing is the enhancement of interlayer adhesion. Under elevated temperature conditions, polymer chain segments gain greater mobility, which leads to their partial diffusion between adjacent layers. In practice, this means stronger "welding" of the layers and a reduction of the natural weak points in the print structure. As a result, the mechanical strength of the components is improved, especially in the direction perpendicular to the layers, where it is typically the lowest [Ngo 2018].

A second significant benefit is the reduction of mechanical property anisotropy. Due to the way FDM models are formed, printed parts exhibit distinct differences in strength depending on the direction of the load. Annealing allows for a partial reduction of these differences through better layer coalescence and more homogeneous material organization. As a result, the printed part exhibits more similar strength parameters in different directions [Gorczynska 2018].

Annealing also influences parameters such as the modulus of elasticity, stiffness, and resistance to permanent deformation. In predominantly amorphous materials, such as ABS, thermal treatment may lead to structural relaxation and changes in mechanical properties and dimensional stability. In semi-crystalline materials, such as polyamides (PA), annealing may additionally promote changes in the crystalline structure, potentially increasing the degree of crystallinity and consequently affecting stiffness and thermal resistance, sometimes at the expense of impact strength. Although PETG is a glycol-modified variant of PET, the incorporation of glycol units disrupts regular chain packing and significantly limits its ability to crystallize. Therefore, changes in the mechanical properties of PETG during annealing should not automatically be attributed to an increase in crystallinity; structural relaxation and the release of residual stresses may also contribute to the observed effects [Sikora 2006, Wrobel 2019].

Annealing can also improve flexural strength and fracture resistance, as the process of internal stress relaxation causes the material to behave more homogeneously under load. The literature describes cases in which properly selected thermal treatment led to a noticeable increase in the strength of elements made of PETG, PLA, or ABS.

However, it is worth emphasizing that the positive effects of annealing are not guaranteed if the process parameters are chosen incorrectly. Too high a temperature can lead to material softening and geometric deformation, while an excessively long annealing time can cause excessive shrinkage or a deterioration of the model's dimensional accuracy. Therefore, this process requires careful adjustment to the type of material used and the intended application of the component [Gorczynska 2018].

The effectiveness of annealing FDM-manufactured components depends primarily on the proper selection of process parameters, such as temperature, holding time, and cooling method. These parameters must be tailored to the properties of the specific material, its molecular structure, and characteristic temperatures, such as the glass transition temperature (Tg) or the melting temperature (Tm). Improper selection of annealing conditions can lead to adverse phenomena, such as deformations, shrinkage, or loss of dimensional accuracy, which is widely described in the literature concerning FDM technology [Ngo 2018, Przybylski 2020].

In engineering practice, the annealing of semi-crystalline materials, which exhibit the ability to reorganize their structure at elevated temperatures, is of particular importance. A good example of such a material is PETG, frequently used in 3D printing due to its favourable mechanical properties, low processing shrinkage, and good interlayer adhesion. PETG typically features a glass transition temperature in the range of 75–85°C, which serves as the basis for determining annealing parameters [Polymaker 2026].

The annealing process for PETG components is most often carried out at temperatures ranging from 70 to 90°C—a level below which the material begins to lose its shape stability, yet high enough to enable internal stress relaxation and partial structural reorganization. In this temperature range, polymer chain segments gain greater mobility, which facilitates the

reduction of stresses and improves interlayer cohesion [Gorczynska 2018, Wrobel 2019].

Annealing time depends on the size and geometry of the component; however, in most cases, it ranges from 30 minutes to 2 hours. Shorter annealing times may be insufficient for full stress relaxation, while an excessively long duration can lead to undesirable dimensional changes or an increase in crystallinity beyond the desired level. Upon completion of the process, slow cooling of the components—ideally within the same heating chamber—is crucial, as it prevents the formation of new thermal gradients and the re-generation of stresses [Przybylski 2020].

Against this background, PETG is considered a dimensionally stable material with relatively good resistance to deformation, making annealing a potentially predictable and widely used post-processing method in engineering applications [Szykiedans 2016, Wrobel 2019].

Materials and Methods

The study investigated the influence of annealing on the mechanical properties of PETG specimens fabricated using fused deposition modeling (FDM). All 84 specimens were manufactured using green Polymaker PETG filament from the same spool on a Snapmaker J1 3D printer using SnapmakerOrca software. This ensured consistency of the filament source and colour across all experimental groups. However, the potential influence of pigments and other colour additives on the mechanical properties was not independently investigated.

The specimens were designed in Siemens NX according to PN-EN ISO 527 (type B1), with an overall length of 150 mm, a narrow-section width of 10 mm, a thickness of 4 mm, and a gauge length of 50 mm. All specimens were positioned flat on the build plate, with their broad faces in contact with the printing surface and their longitudinal axes parallel to each other. The specimens were arranged side by side in the same horizontal plane, using the same orientation for all four infill density variants (25%, 50%, 75%, and 100%).

The printing parameters were kept constant: a nozzle diameter of 0.4 mm, a nozzle temperature of 255°C, a build plate temperature of 70°C, and a layer height of 0.2 mm. Each specimen was printed with two wall perimeters, four top and bottom layers, and a rectilinear infill pattern. The internal structures of the specimens are presented in Figure 2.

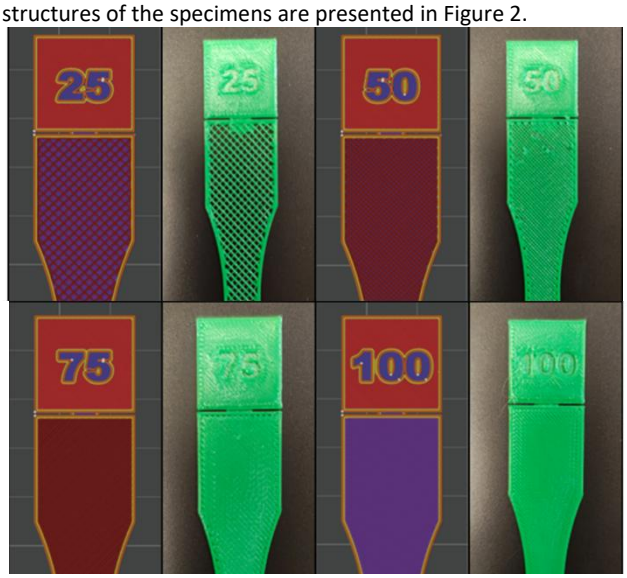


Figure 2. Presentation of the density of slicer model and sample fillings (25–100%).

1.1 Annealing Process

Following the printing process, the specimens were subjected to an annealing treatment in a laboratory convection furnace. The samples were categorized into three experimental groups (Tab. 1) to assess the impact of thermal history: Group A (Control): Untreated specimens, used as a reference. Group B and C: Specimens annealed at 90°C, 100°C, and 110°C. After reaching the target temperature, samples were held for 30 minutes to ensure thermal stabilization. Two cooling strategies were applied (Fig. 3): Group B: slow cooling within the furnace (~2 h) and Group C: rapid cooling under ambient conditions (~21°C). The temperatures were chosen as it exceeds the glass transition temperature (80°C) of the PETG material, facilitating polymer chain relaxation without causing excessive geometric distortion.

Annealing Temp.	Cooling Method	25%	50%	75%	100%
Control	N/A	N	N	N	N
90°C	Furnace	N	N	N	N
90°C	Ambient	N	N	N	N
100°C	Furnace	N	N	N	N
100°C	Ambient	N	N	N	N
110°C	Furnace	N	N	N	N
110°C	Ambient	N	N	N	N

Table 1. Number of specimens per test variant (N=3 for each condition). "Furnace" indicates controlled cooling inside the furnace; "Ambient" indicates cooling outside the furnace.

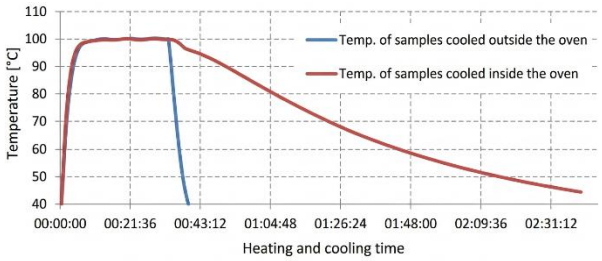


Figure 3. Temperature profiles recorded using a thermocouple positioned inside a specimen during two separate cooling trials following annealing at 100°C: cooling inside the furnace and cooling under ambient conditions outside the furnace.



Figure 4. Specimens inside the furnace during annealing, including the specimen prepared for internal thermocouple measurements [own study].



Figure 5. Thermographic image of specimens during cooling under ambient conditions after annealing.

To verify that the specimens were subjected to heat treatment at the intended duration and temperature, one of the samples was equipped with a thermocouple (Fig. 4) connected to a National Instruments cDAQ-9171 chassis and an NI TB-9212 terminal block. Real-time recording and monitoring were conducted using NI SignalExpress 2015 software. The integration of internal thermocouple measurements and external thermal imaging (Fig. 5) confirmed that the material effectively reached the desired temperature, facilitating uniform polymer chain relaxation while minimizing the risk of localized thermal degradation or excessive deformation.

1.2 Mechanical Testing

Static tensile tests were performed using a Zwick/Roell Z100 universal testing machine controlled by testXpert II software. The test parameters included the specimen dimensions, an initial grip-to-grip distance of 100 mm, a preload of 0.1 MPa, and a test speed of 50 mm/min. All specimens were tested until failure, and the results were exported to Microsoft Excel for further analysis. No necking was observed during testing.

The ultimate tensile strength was calculated as the maximum tensile force divided by the estimated load-bearing cross-sectional area:

$$Rm = \frac{F_{max}}{A}$$

Where (Fmax) is the maximum tensile force and (A) is the estimated cross-sectional area of the deposited material, determined individually for each specimen from the slicer-defined geometry. The estimation accounted for the outer perimeters and infill paths, based on the layer height and extrusion line width.

A total of 84 specimens were tested, comprising 72 annealed specimens and 12 untreated reference specimens. Three specimens were tested for each specific experimental condition (n = 3). The primary objective was to evaluate changes in ultimate tensile strength (UTS) and elongation at break to assess the effects of annealing on the mechanical properties of FDM-printed PETG specimens.

Infrared thermography was used during tensile testing to record temperature changes on the specimen surface throughout deformation and fracture. Selected frames extracted from the recorded thermal video were used to illustrate the temperature distribution at specific stages of the test. Post-fracture observations were also used to characterize failure modes and examine their relationship with the processing parameters.

2 RESULTS AND DISCUSSION

On the thermograms presented in Figure 6, significant differences can be observed in how loads are transferred by specimens with varying infill levels. In specimens with a low infill degree (e.g., 25%), areas of elevated temperature align with the orientation of material paths, indicating that tensile forces propagate primarily along the geometric layout of the infill. The location of thermal zones demonstrates that deformations are concentrated in areas with lower structural continuity, and the deformation process is highly anisotropic. Consequently, deformation planes emerge with an oblique or irregular trajectory, determined by the internal geometry of the specimen.

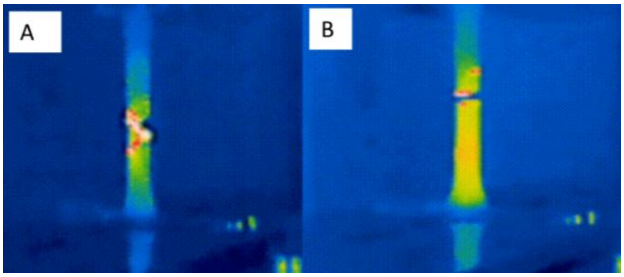


Figure 6. Thermogram during the tearing of samples with filling A-25% and B-100%.

A different behavior was recorded for the 100% infill specimen. The uniform structure of the material leads to a more even distribution of loads, which results in the distinct formation of a narrow temperature increase zone. This area corresponds to the failure initiation plane, the trajectory of which is approximately perpendicular to the direction of the applied tensile force. This mode of crack propagation is typical for materials with increased homogeneity, where there are no internal discontinuities that would influence local stress concentration.

Infrared thermography revealed localized temperature increases in regions of maximum strain, corresponding to zones of plastic deformation and crack initiation. The observed thermal patterns confirm the conversion of mechanical work into heat and provide insight into the failure process.

Strain localization was more pronounced in high-infill samples, whereas lower infill structures exhibited more distributed deformation due to their heterogeneous internal architecture. Cracks predominantly initiated at interlayer interfaces and propagated along filament deposition paths, confirming the anisotropic nature of FDM-produced materials. Higher infill specimens showed mixed-mode fracture behaviour, while lower infill samples exhibited more ductile characteristics associated with progressive deformation (Figure 7).

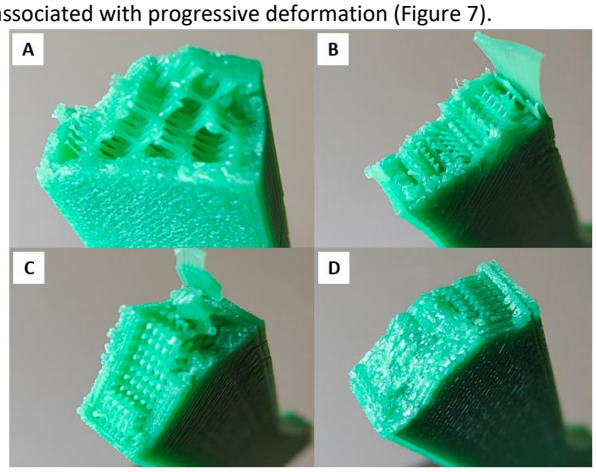


Figure 7. Appearance of the sample cross-section after fracture. A-25%, B-50%, C-75%, D-100%.

Annealing induced measurable dimensional changes, particularly shrinkage along the build direction (Z-axis). These effects are attributed to stress relaxation and polymer chain rearrangement during thermal exposure. The magnitude of deformation depended on infill density and cooling conditions. Fractographic observations indicate that failure mechanisms are strongly dependent on internal structure.

According to the results presented in Figure 8., the shrinkage value of the height (H) increased systematically with the annealing temperature and was particularly evident for samples cooled in the oven, reaching over 4%. Simultaneously, the shrinkage of the width (B) took on negative values, which indicated a reduction in dimension B after annealing; these changes ranged from −0.8% to −2.75%. Specimens with 100% infill showed the greatest dimensional stability, which is consistent with their compact and least porous structure.

The observed differences in the shrinkage of both dimensions clearly confirm the anisotropy characteristic of FDM technology. The height of the specimens (H) corresponds to the layer-building direction, which is the most susceptible to stress relaxation and polymer structure reorganization during annealing. In this direction, the material has a greater share of inter-layer micro-gaps and lower adhesive cohesion, which is why the annealing process leads to their partial closure and, consequently, to noticeable shrinkage. The width dimension (B), corresponding to the direction in the XY plane, is characterized by significantly higher homogeneity and a better degree of fusion of deposition lines, which limits the scale of thermal deformations. Negative shrinkage of B indicates that annealing mainly caused a densification of the existing structure in the layer plane, though to a significantly lesser degree than in the Z direction. Thus, the disparity between the shrinkage of H and B clearly reflects the directional nature of the mechanics of material produced by additive technology. The smallest shrinkage anisotropy occurred in specimens with 100% infill, which results from the reduction of internal voids and an increase in structural continuity. Specimens with lower infill showed greater differences between the shrinkage of H and B, which indicates that internal porosity intensifies the effect of directional deformation.

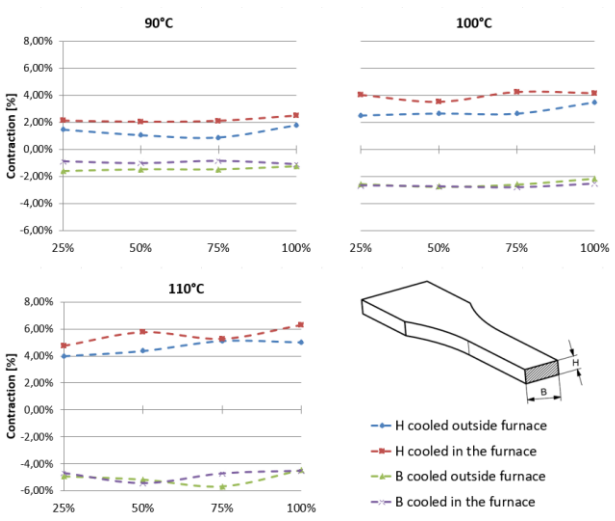


Figure 8. Sample contraction after cooling.

Dimensional changes resulting from annealing were evaluated by measuring the specimen width (B) and thickness (H) with a caliper in the fracture region. Although the nominal cross-sectional dimensions specified in the CAD model were 10 mm × 4 mm, the as-printed specimens did not perfectly reproduce these dimensions. Therefore, dimensional changes were calculated relative to the actual dimensions measured before heat treatment. Negative percentage values indicate dimensional reduction (shrinkage), whereas positive values indicate dimensional expansion.

$$S = \frac{D_1 - D_0}{D_0} \times 100\%$$

S - relative dimensional change [%],
D_0 - actual dimension before heat treatment,
D_1 - dimension after heat treatment.

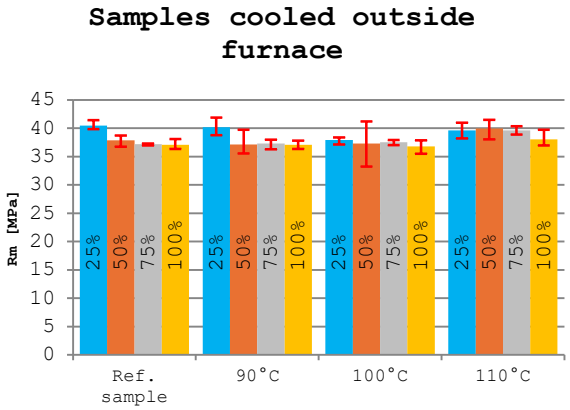
The tensile properties exhibited a dependence on infill density. Specimens with 75% and 100% infill generally demonstrated higher tensile strength and stiffness, whereas specimens with 25% infill showed reduced load-bearing capacity and greater variability due to structural discontinuities (Fig. 9). The columns represent the mean tensile strength values for each experimental condition, while the error bars indicate the range between the minimum and maximum measured values among the three specimens tested under each condition (n = 3).

Annealing at 100°C resulted in relatively high tensile strength values, suggesting that this temperature may promote stress relaxation and improve interlayer bonding. However, increasing the temperature to 110°C did not produce a consistent further improvement across all infill densities.

Cooling conditions also influenced the measured tensile strength. Furnace-cooled specimens generally exhibited less variation under some experimental conditions, whereas air-cooled specimens showed a wider range of values in certain cases (Fig. 9). These observations indicate that the effects of annealing temperature and cooling method depend on the infill density and should be interpreted in relation to the measured variability.

Collective plots reveal significant differences in the effects of annealing based on temperature, cooling method, and infill density. The greatest strength increases were recorded for specimens: cooled in the oven, annealed at 110°C, with 100% infill. Specimens with lower infill showed a limited response to annealing, which can be attributed to a more porous, less compact structure.

The analysis of tensile strength increase (Fig. 10) shows clear differences in the behaviour of samples with various infill degrees during oven annealing and cooling. The lines corresponding to 100% and 50% infill are exceptionally clear: as the temperature rises, the Rm increase grows stably without sudden drops or deviations.



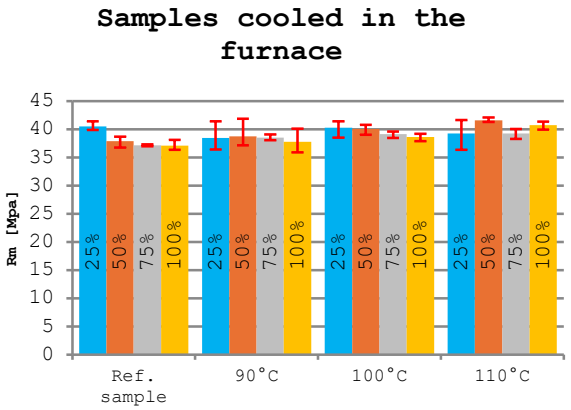
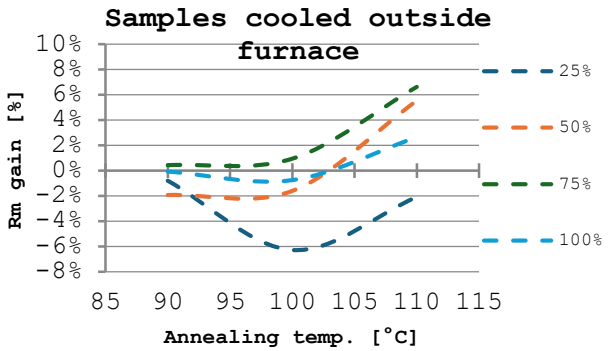


Figure 9. Comparison of tensile strength after annealing, with filling increasing from 25 to 100%.

This progression suggests that the structure of these specimens is morphologically homogeneous, and the continuity of the polymer phase ensures effective heat conduction and uniform relaxation of stresses generated during the printing process. Samples with 75% and 25% infill behave quite differently. Their curves in Figure 10 are significantly less orderly—more flattened and locally irregular.

This instability is not coincidental. The 75% infill is at the boundary between a compact body and a porous structure, which leads to local differences in heat transport and hinders the uniform segmental reorganization of PETG chains during annealing. In practice, this means the material "reacts" to heat treatment fragmentarily rather than in a coordinated manner.

Furthermore, the results presented clearly show that 25% infill samples react to annealing quite differently than samples with higher material density. While the 50%, 75%, and 100% series show a systematic increase in Rm values with higher annealing temperatures and slow oven cooling, the 25% samples record a decrease in Rm compared to reference samples, particularly when annealed and cooled in the oven. This phenomenon results from their exceptionally porous, highly shell-like geometry. In 25% samples, the load is carried almost exclusively by the perimeters, which maintain a favourable molecular orientation resulting from the extrusion process before annealing.



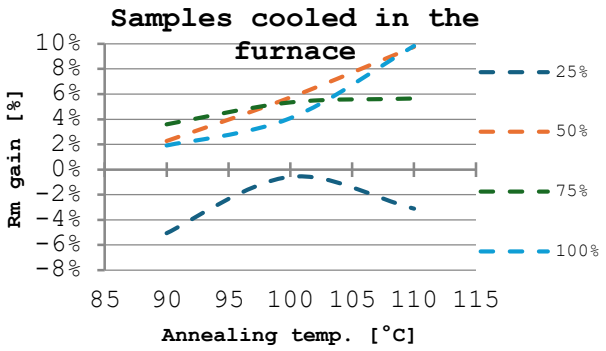


Figure 10. Increase in tensile strength of samples after annealing.

The decrease in tensile strength Rm observed in some specimens with 25% infill after annealing may be associated with their relatively sparse internal structure and the increased mobility of polymer chain segments at temperatures near or above the glass transition temperature (Tg) of PETG. Possible effects include the relaxation of residual stresses introduced during FDM printing and changes in the local structure of the deposited material and interlayer regions. However, these mechanisms were not directly investigated in the present study and should therefore be regarded as possible explanations of the measured mechanical response. No direct conclusions regarding changes in crystallinity or molecular orientation can be drawn from the tensile tests and dimensional measurements alone.

A comparative analysis of the percentage increase in tensile strength confirmed that controlled cooling enhances repeatability and mechanical stability. For solid specimens, the most unambiguous improvement in tensile strength was observed, particularly at a temperature of 110°C, where mean values exceeded 40 MPa. These results confirm that full infill combined with slow cooling allows for the maximum utilization of the structural stabilization effect of PETG.

3 CONCLUSIONS

The objective of this study was to determine the extent to which annealing affects the mechanical properties of PETG prints manufactured using FDM technology. The theoretical section discussed phenomena characteristic of FDM technology, such as anisotropy and residual stress, as well as the mechanism of improving interlayer bonding during heat treatment. In the experimental section, specimens with four infill densities (25%, 50%, 75%, and 100%) were prepared and subjected to annealing at three temperatures: 90°C, 100°C, and 110°C, using two different cooling variants.

Untreated specimens exhibited mean tensile strengths of 40.49 MPa, 37.89 MPa, 37.18 MPa, and 37.09 MPa for infill densities of 25%, 50%, 75%, and 100%, respectively. Tensile strength was calculated using an estimated load-bearing cross-sectional area determined individually for each specimen based on the slicer-defined geometry, taking into account the outer perimeters, infill paths, layer height, and extrusion line width. Thus, the calculation did not assume a uniform nominal cross-sectional area of 40 mm² for all specimens. For example, the estimated area of a 25% infill reference specimen was 24.1257 mm². The relatively high tensile strength measured for the 25% infill specimens may therefore reflect, in part, the use of the estimated material-bearing cross-sectional area in the stress calculation. The contribution of the continuous outer perimeters to load transfer may also be relevant, although this mechanism was not independently verified.

After annealing, changes in properties were strongly dependent on the infill degree. In the case of 25% infill

specimens, mean tensile strength values remained at the level of 38–40 MPa, i.e., very close to the reference specimens, which indicates limited potential for strength improvement under the investigated annealing conditions. More pronounced differences were observed for 50% and 75% infill. For example, specimen W16 (50%, annealed at 100°C) reached 41.19 MPa, a value comparable to the highest results obtained for untreated specimens. For 75% infill, mean tensile strength values after annealing remained at the level of 37–39 MPa; however, other parameters changed significantly, in particular, the elongation at break, which in some cases exceeded 11%. In the case of solid (100% infill) specimens, tensile strength remained relatively stable before and after annealing, within the range of 37–41 MPa, indicating limited changes in strength under the investigated conditions. These trends were also reflected in the averaged results charts.

An essential element of the experiment was also a thermographic analysis of the tensile test. Thermographic images clearly showed the location of areas with the highest temperature, corresponding to the sites of greatest deformation. This confirmed that the mode of force transfer in elements made by the FDM method is strongly related to the layout of layers and interlayer connections—a phenomenon that was particularly pronounced in specimens with lower infill. Based on the literature and the obtained research results, the following conclusions were drawn: Annealing affects the mechanical properties of PETG specimens, but its effects are clearly dependent on the infill degree. 25% infill specimens showed no significant changes (mean Rm: 38–40 MPa), while at 50% infill, an increase in strength to values as high as 41.19 MPa (W16) was recorded. 75% and 100% infill variants were characterized by greater parameter stability, although noticeable changes in elongation at break appeared in some specimens. The greatest benefits were brought by annealing at 100°C. This value corresponds to the glass transition temperature of PETG, which confirms the theoretical assumptions regarding the mobility of polymer chain segments. Results at 110°C did not bring further improvement—mean Rm values remained at the level of 37–40 MPa, and local drops in other parameters were observed. Cooling in the oven promotes dimensional stability and structural homogeneity. In specimens cooled at ambient temperature, greater differences in deformation parameters appeared, which could result from an uneven temperature gradient during cooling. Annealing effectively reduces internal stresses, but it also causes material shrinkage, which was noted during dimensional measurements. This phenomenon should be taken into account in elements requiring strict dimensional tolerance. Thermographic studies revealed the mechanism of local stress concentration during stretching. Areas with the highest temperature, visible on thermograms, coincided with the places of subsequent specimen failure. This is consistent with the characteristics of FDM prints, in which interlayer connections constitute natural "paths" for directing deformations. Non-annealed specimens with low infill (25%) showed higher nominal tensile strength than specimens filled at 100%, which results from the dominance of perimeters working as thin-walled elements. In non-annealed specimens, i.e., those not subjected to heat treatment improving interlayer bonding, the solid structure reveals lower core microstructure quality—numerous weak connections between filaments favour crack initiation and lower the effective load-bearing capacity of the cross-section. The results confirm that in FDM technology, strength is determined not by the amount of material, but by the continuity and quality of paths transferring loads. As a result of the obtained findings, it can be stated that the hypothesis proposed in the work was confirmed, though not in the full range. Annealing indeed contributed to stress relaxation and improvement of structural homogeneity, which was particularly visible at 100°C and in specimens with medium infill. However, an increase in mechanical strength occurred primarily for the 50% infill, whereas for the other variants, changes concerned mainly the mode of deformation, not the Rm value itself. This means that the effectiveness of annealing depends both on the temperature and the internal geometry of the specimen, which partially limits the scope of the hypothesis confirmation. Despite this, the general direction of the observed changes confirms that properly selected heat treatment parameters can beneficially affect the properties of PETG prints, while simultaneously taking into account the accompanying shrinkage. In light of the obtained results, it would be reasonable to: expand research to include analysis of Young's modulus and fatigue resistance, conduct microstructural studies (e.g., SEM) allowing for the assessment of the quality of interlayer welds after annealing, investigate the influence of different cooling rates—not only extreme variants, compare results with a numerical deformation model, perform tests for other geometries and infill layouts, compare PETG with materials with a higher degree of crystallinity (e.g., PA). Expanding research to include the above aspects will enable a fuller understanding of processes related to the annealing of 3D prints and will allow for better utilization of this technology in practical engineering applications.

CONTACTS:

Eng. Marcin Marciniak PhD.
MSc Eng. Jacek Ochorok
Rzeszów University of Technology,
The Faculty of Mechanics and Technology,
Kwiatkowskiego 4, 37-450 Stalowa Wola, Poland, +48668357211, m.marciniak@prz.edu.pl, wmt.prz.edu.pl

REFERENCES

[Adamczyk 2020] Adamczyk, K., Dróżdż, E., Łopata, N., Pałka, K. Technologie AM i rapid prototyping. Gliwice: Politechnika Śląska, 2020.

[ASTM 2009] ASTM. Additive Manufacturing Terminology. 2009.

[ASTM/ISO 2021] ASTM/ISO. Terminologia i klasyfikacja procesów AM (ASTM F2792, ISO/ASTM 52900). Available from: https://webstore.ansi.org/standards/astm/ASTME1527E1528Environmental

[AutomatykaOnline 2021] Łukasiewicz – PIAP. Metody wytwarzania przyrostowego. AutomatykaOnline, 2021. Available from: https://automatykaonline.pl/Artykuly/Druk-3D/Metody-wytwarzania-przyrostowego [25.01.2026].

[Duda 2016] Duda, T., Raghavan, L. V. 3D printing technologies, materials, and applications. IFAC-PapersOnLine, 2016, Vol. 49, No. 29.

[Gibson 2021] Gibson, I., Rosen, D., Stucker, B. Additive Manufacturing Technologies: 3D Printing, Rapid Prototyping, and Direct Digital Manufacturing. Springer, 2021.

[Gorczynska 2018] Górczyńska, A., Żenkiewicz, M. Polimery stosowane w technikach przyrostowych - właściwości i możliwości zastosowania. Polimery, 2018.

[Mikos 2021] Mikoś, J. Przegląd technologii druku 3D jako produkcji dodatkowej do wykonywania prototypów

małych maszyn elektrycznych. Maszyny Elektryczne, Zeszyty Problemowe, 2021, nr 2 (126).

[Ngo 2018] Ngo, T. D., Kashani, A., Imbalzano, G., Nguyen, K. T. Q., Hui, D. Additive manufacturing (3D printing): A review of materials, methods, applications and challenges. Composites Part B: Engineering, 2018, Vol. 143, pp. 172–196.

[PETG 2026] PETG filament technical data sheets. 2026.

[Polymaker 2026] Polymaker. Available from: https://polymaker.com [25.01.2026].

[Przybylski 2020] Przybylski, W. Technologie przyrostowe. Druk 3D i jego zastosowania w inżynierii. Warszawa: PWN, 2020.

[Sikora 2006] Sikora, R. Przetwórstwo tworzyw polimerowych. Lublin: Wydawnictwo Politechniki Lubelskiej, 2006.

[Styp 2020] Styp-Rekowski, M., Matuszewski, M., Oborski, I., Polishchuk, O. Miejsce technik przyrostowych w procesach wytwórczych. Obróbka Metalu (Fuchs Oil), 2020, nr 41.

[Szykiedans 2016] Szykiedans, K., Credo, W. Mechanical Properties of FDM and SLA Low-cost 3-D Prints. Procedia Engineering, 2016, Vol. 136, pp. 257–262. Available from: https://www.researchgate.net/publication/293043879 [25.01.2026].

[Szymczyk 2017] Szymczyk, E. Badanie właściwości mechanicznych elementów wytwarzanych metodą FDM. Postępy Nauki i Techniki, 2017.

[Wohlers 2022] Wohlers, T. Wohlers Report 2022: 3D Printing and Additive Manufacturing State of the Industry. Wohlers Associates, 2022.

[Wrobel 2019] Wróbel, A. Materiały polimerowe w technikach addytywnych. Mechanik, 2019.

LICENSE CREATIVE COMMONS:

The article is published under the terms and conditions of the Creative Commons Attribution 4.0 International License (CC BY 4.0).